Coastal Marine Science 32(3): 000–000, 2009

Cohesive sediment transport in the 3D-hydrodynamic-baroclinic circulation model in the Mahakam Estuary, East Kalimantan, Indonesia

Idris MANDANG[1,2] and Tetsuo YANAGI[3]

[1] *Interdisciplinary Graduate School of Engineering Science, Kyushu University, Kasuga 816-8580, Japan*
E-mail: idris@riam.kyushu-u.ac.jp, idris_mdg@yahoo.com
[2] *Faculty of Science Mulawarman University, Indonesia*
[3] *Research Institute for Applied Mechanics, Kyushu University, Kasuga 816-8580, Japan*

Received: 29 January 2008; Accepted 18 July 2008

Abstract—A fully three-dimensional finite difference baroclinic model system for hydrodynamics and cohesive sediment transport is described. The hydrodynamic model is based on the hydrostatic and Boussinesq approximations. The simulation of cohesive sediment transport processes is performed solving the 3D-conservative advection-diffusion equation. The model is ECOMSED (Estuarine Coastal and Ocean Modeling System with Sediment) developed by HydroQual, Inc., (2002) which is applied to the transport of cohesive sediments in the Mahakam Estuary, East Kalimantan, Indonesia. The model was run for 15 days (27 June–12 July 2000) driven by tidal forcing at the open boundary and river discharge at the upstream. The observed temperature, salinity, and suspended sediment data were available for the start of the simulation. Good agreement was found between model results and observed temporal and spatial variations in water elevation, currents, and suspended sediment concentration (SSC) in the Mahakam Estuary. During the flood tidal condition, the tidal current advected the higher salinity water into the estuary, resulting in a relatively large salinity gradient inside the estuary. During the ebb tidal condition, the combined gravitational and tidal flows moved the low salinity water seaward from the upstream, leading to a rapid decrease of salinity near the mouth of the estuary. The simulation results of suspended sediment transport in the Mahakam Estuary nearly followed the salinity transport. The suspended sediments were mainly transported from Mahakam river towards Muara Pegah and Muara Jawa than Muara Berau and Muara Bayur. The SSC at Muara Jawa, Muara Pegah, and Muara Kaeli was mainly influenced by river discharge, meanwhile at Muara Bayur it was dominated by tidal current.

Key words: numerical models, baroclinic, salt wedge, Estuary of Mahakam Delta, tide, cohesive sediment transport, river discharge

Introduction

The Mahakam Delta, located on the east coast of Kalimantan, Indonesia, is an active delta system which has been formed in humid tropical environment under condition of relatively large tidal amplitude, low wave-energy, and large fluvial input (Fig. 1(a)). Tidal processes control the sediment distribution in the delta mouth and are responsible for the flaring estuarine-type inlets and numerous tidal flats.

The present Mahakam river drains about 75,000 km^2 of the Kutei Basin shown in Fig. 1(a), which is a part of the uplifting central Kalimantan ranges. From available rainfall data and the size of the drainage basin, a mean water discharge was evaluated as the order of value ranging from 1800 to 2800 $m^3 s^{-1}$ with large seasonal variations (Allen and Chambers, 1998). Floods up to 5000 $m^3 s^{-1}$ may occur in the upper and middle reaches of the catchment, which is separated from the river mouth by a subsiding area characterized by a low relief alluvial plain and several large lakes, located about 150 km upstream of the delta plain (Roberts and Sydow, 2003). The lakes create a buffer causing the damping of the flood surges (Storms et al., 2005) and effectively level the Mahakam river floods, resulting in a constant discharge for lower reaches of the Mahakam river and delta system. The absence of peaks in river discharge has resulted in a delta plain that neither features natural levees or crevasse splays, and avulsions of disributary of channels have never taken place (Storm et al,. 2005). As the delta prograded, bifurcations of the fluvial distributaries occurred about every 10 km. The channels in the Mahakam river have variable depths generally ranging between 3 and 12 m.

The modern Mahakam delta has two active fluvial distributary system directed northeast and southeast. The intervening areas consist of tide dominated areas, with many high sinuosity channels which are mostly not connected to the flu-

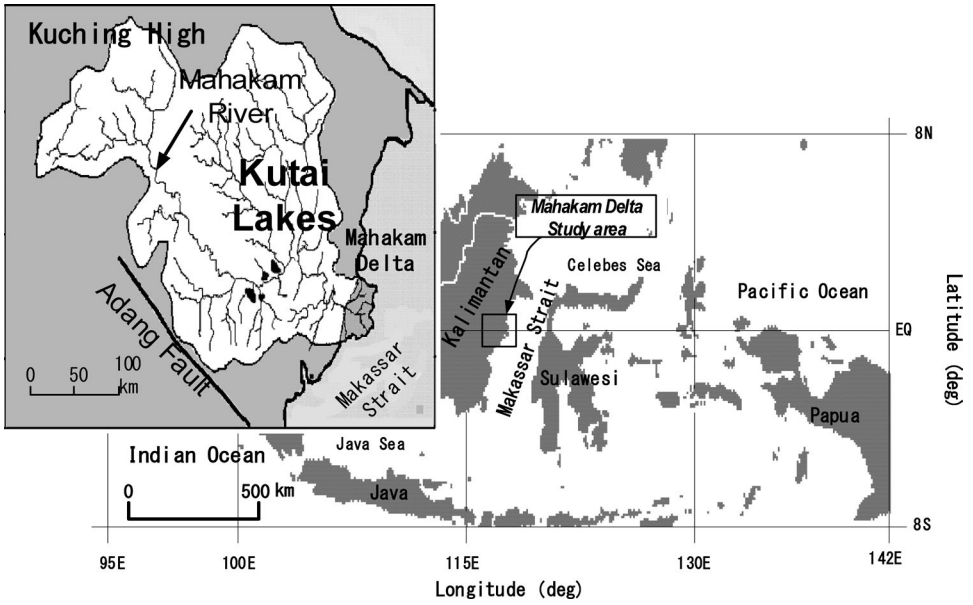

Fig. 1(a). Location map of the Mahakam Delta (study area) on the east of Kalimantan, Indonesia and Mahakam river drainage basin (Allen and Chambers, 1998).

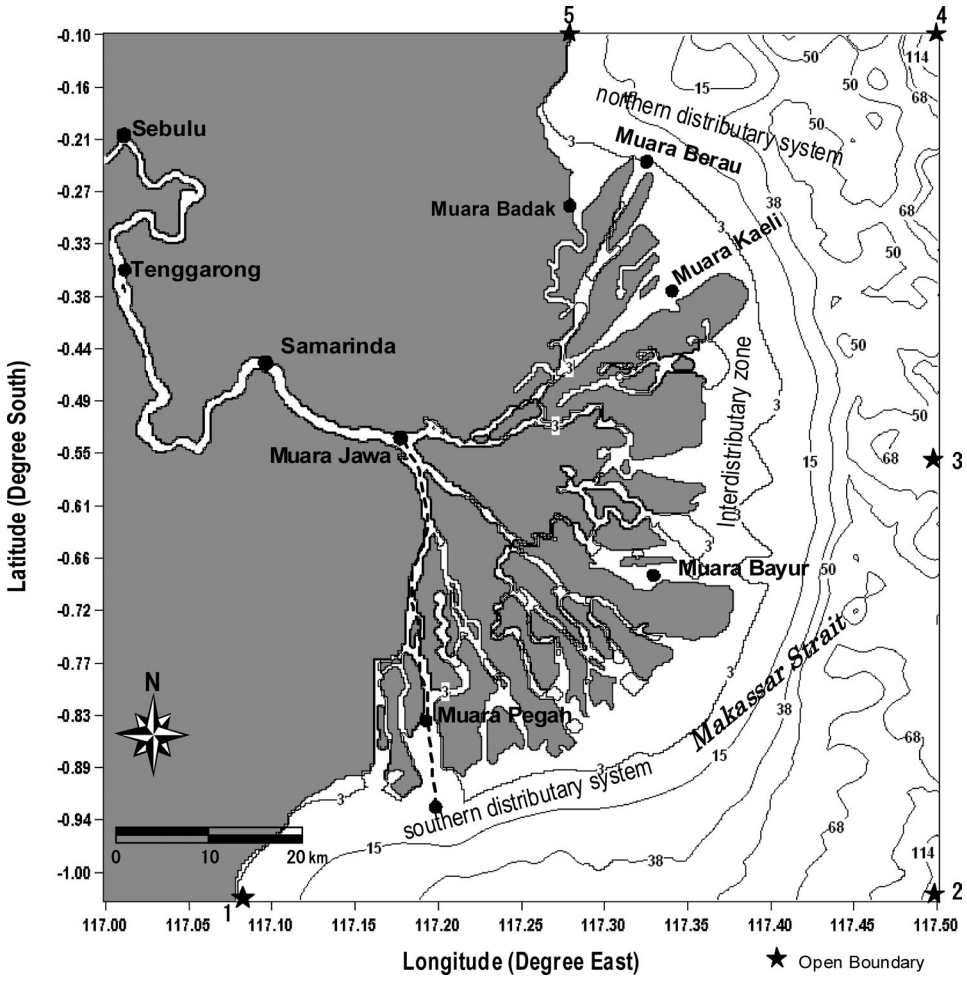

Fig. 1(b). Bathymetric map of the Mahakam Estuary from DISHIDROS of Indonesian Navy and the locations of the transect (broken line). Numbers show the depth in meters. Stars show the stations for open boundary, which are shown in Table. 1.

vial system (Fig. 1(b)). This intredistributary zone occupies approximately 30% of the delta plain (Allen et al., 1977).

The scope of this study is to implement and expand the hydrodynamic numerical modeling system to accommodate these density driven flows for estuarine zone. The model used is fully integrated three dimensional (3-D), time dependent, hydrodynamic, and sediment transport. This module of ECOMSED (Estuarine Coastal and Ocean Modeling System with Sediment), developed by HydroQual, Inc., (2002), has been successfully applied to the coastal and estuarine waters. The development of ECOMSED was originated in the mid 1980's with the creation of the Princeton Ocean Model (Blumberg and Mellor, 1987). Some recent applications of the module include Chesapeake Bay (Blumberg and Goodrich, 1990), Delaware Bay and Delaware River (Galperin and Mellor, 1990), the Gulf Stream Region (Ezer and Mellor, 1992). Mandang and Yanagi (2008) well reproduced the tides and tidal currents with the use of a horizontally two-dimensional barotropic hydrodynamical model ECOMSED which was applied to the Estuary of Mahakam Delta, East Kalimantan, Indonesia.

The objective of this study is to identify the circulation pattern of the water and sediment transport in an estuarine zone of Mahakam Delta.

Materials and Methods

Observation data

Bathymetry data of the model domain were obtained from DISHIDROS (Indonesian Navy Hydrographic Department) of Indonesian Navy. The model domain in this study covers the area of Mahakam Delta (0°10′00″S–1°03′00″S and 116°59′00″E–117°49′14″E), offshore area of approximately 30 km from Muara Bayur toward the Makassar Strait and from Muara Pegah up to Sebulu which passes through the Samarinda city (Fig. 1(b)).

Time series of water surface elevation, current velocity, and suspended sediment concentration (SSC) data were obtained by the IMAU (Institute for Marine and Atmospheric Research Utrecht University, the Netherland) which conducted the field observation in the Mahakam Delta during the period of 30 June–8 July 2003 (the southeast monsoon). Water surface elevation and current velocity were measured using a pressure sensor and ADCP (the Acoustic Doppler Current Profiler), respectively. The SSC was measured by seapoint Optical Backscatter Sensor (OBS) which was attached to the CTD (*Conductivity*, *Temperature*, and *Depth*) probe. The time series data were sampled at only one station at Muara Jawa (Fig. 1(b)) at the depth of 4.0 m from the surface and utilized to verify and validate the model results.

The transects of temperature, salinity, and suspended sediment data were obtained by the IMAU along the line shown by dotted line in Fig. 1(b). These variables were measured with a CTD. The CTD was lowered and raised in the water, meanwhile the CTD took readings of the pressure, conductivity and temperature, an extra OBS sensor recorded the backscatter of an optical signal against suspended sediment.

Model description

The ECOMSED model is a three-dimensional hydrodynamic and sediment transport model. The governing equations of the hydrodynamic component in the model are the continuity equation, momentum equation, and heat and salt transport equations. The simulation of cohesive sediment transport processes is performed solving the 3D-conservative advection-diffusion equation. The hydrodynamic governing equations are solved using a mode-splitting technique. The external mode that contains fast moving gravity wave is solved with small time step to ensure stability, whereas the internal mode uses large time step to save the computation time. Finite difference of the differential equation is applied on a staggered C grid in space, and the three-time-level leapfrog scheme is applied for the time stepping. Three schemes, including central difference, upwind difference, and the multidimensional positive definite advection scheme are provided in the model to solve the advection term in the transport equations. The sediment transport component uses the same grid, structure, and computational framework as the hydrodynamic component to simulate the settling, deposition, and resuspension of cohesive sediments.

Hydrodynamic Model

The Governing equations

The hydrodynamic part of the model uses the following basic equations. The basic equations for the three-dimensional mode are:

The continuity equations:

$$\frac{\partial U}{\partial x}+\frac{\partial V}{\partial y}+\frac{\partial W}{\partial z}=0\,, \tag{1}$$

where (U,V,W) are the eastward (z), northward (y), and upward (z) components of the current. A dynamic boundary condition evaluated at the sea surface $z=\eta$ will indicate the relation between sea surface elevation η and vertical velocity at the sea surface W_η as,

$$\frac{\partial \eta}{\partial t}+\frac{\partial \eta}{\partial x}U_\eta+\frac{\partial \eta}{\partial y}V_\eta=W_\eta\,, \tag{2}$$

The vertical velocity at the sea surface W_η can be obtained by integrating (1) from the bottom $z=-H$ to the sea surface $z=\eta$.

The momentum equations using the Boussinesq approximations and the assumption of vertical hydrostatic equilibrium in Cartesian coordinates are given below.

$$\frac{\partial U}{\partial t}+U\frac{\partial U}{\partial x}+V\frac{\partial U}{\partial y}+W\frac{\partial U}{\partial z}-fV = -\frac{1}{\rho_0}\frac{\partial P}{\partial x}+\frac{\partial}{\partial z}\left(A_V\frac{\partial U}{\partial z}\right)+\frac{\partial}{\partial x}\left(2A_M\frac{\partial U}{\partial x}\right)+\frac{\partial}{\partial y}\left(A_M\left(\frac{\partial U}{\partial y}+\frac{\partial V}{\partial x}\right)\right), \quad (3)$$

$$\frac{\partial V}{\partial t}+U\frac{\partial V}{\partial x}+V\frac{\partial V}{\partial y}+W\frac{\partial V}{\partial z}+fU = -\frac{1}{\rho_0}\frac{\partial P}{\partial y}+\frac{\partial}{\partial z}\left(A_V\frac{\partial V}{\partial z}\right)+\frac{\partial}{\partial x}\left(A_M\left(\frac{\partial U}{\partial y}+\frac{\partial V}{\partial x}\right)\right)+\frac{\partial}{\partial y}\left(2A_M\frac{\partial V}{\partial x}\right), \quad (4)$$

$$P=\rho_0 g\eta+\rho_0\int_{-z}^{0}B dz, \quad (5)$$

$$B=\frac{\rho-\rho_0}{\rho_0}g, \quad (6)$$

and, the equations of temperature and salinity,

$$\frac{\partial T}{\partial t}+U\frac{\partial T}{\partial x}+V\frac{\partial T}{\partial y}+W\frac{\partial T}{\partial z} = \frac{\partial}{\partial z}\left(K_V\frac{\partial T}{\partial z}\right)+\frac{\partial}{\partial x}\left(A_H\frac{\partial T}{\partial x}\right) \quad (7)$$

$$+\frac{\partial}{\partial y}\left(A_H\frac{\partial T}{\partial y}\right), \quad (8)$$

where T denotes the temperature, S the salinity, f the Coriolis parameter ($=2\Omega\sin\phi$; $\Omega=7.27\times10^{-5}\,s^{-1}$ and ϕ is the latitude), ρ the density, ρ_0 the reference density ($=1024.78\,kg\,m^{-3}$), g the acceleration of gravity ($=9.8\,m\,s^{-2}$), P the pressure, B the buoyancy, A_V and K_V the vertical eddy viscosity and vertical diffusion coefficient, A_M the horizontal eddy viscosity, AH the horizontal diffusion coefficient.

The horizontal eddy viscosity and diffusivity coefficient is given on the basis of Smagorinsky formula where they increase proportionally to the grid spacing and the velocity shear.

$$A_M=A_H=\alpha\Delta x\Delta y\left[\left(\frac{\partial U}{\partial x}\right)+\left(\frac{\partial V}{\partial y}+\frac{\partial U}{\partial y}\right)^2\Big/2+\left(\frac{\partial V}{\partial y}\right)^2\right]^{1/2}, \quad (9)$$

where α is a constant ($=0.22$) and Δx and Δy are horizontal mesh size ($\Delta x=\Delta y=200\,m$).

The vertical eddy diffusivity coefficients of momentum, temperature, salinity, and suspended sediment concentration are obtained through the 2.5 level turbulence closure scheme developed by Mellor and Yamada (1982).

Suspended Sediment Transport Model

The transport equation

The transport of suspended sediment is described by the following advection-diffusion equation:

$$\frac{\partial C}{\partial t}+\frac{\partial UC}{\partial x}+\frac{\partial VC}{\partial y}+\frac{\partial (W-W_s)C}{\partial z} = \frac{\partial}{\partial x}\left(A_H\frac{\partial C}{\partial x}\right)+\frac{\partial}{\partial y}\left(A_H\frac{\partial C}{\partial y}\right)+\frac{\partial}{\partial z}\left(K_V\frac{\partial C}{\partial z}\right) \quad (10)$$

where C denotes suspended sediment concentration, W_s is settling velocity of the cohesive sediment ($cm\,s^{-1}$) which will be shown later.

Bottom shear stress computation

The bed shear stress is computed as follows :

$$\tau_h=\rho u_+^2 \quad (11)$$

where ρ denotes density of the suspending medium ($=2650\,kg\,m^{-3}$), and u_+ a shear velocity.

The shear velocity is defined by the Prandtl-von Karman logarithmic velocity profile

$$u_+=\frac{ku}{\ln\left(\frac{z}{z_0}\right)} \quad (12)$$

where k is von Karman constant ($\cong0.40$), u resultant near bed velocity, z depth at the center of the bottom layer, and z_0 bottom friction specified as input to the model ($=0.001\,m$).

The erosion model

Erodibility of a cohesive bed is driven by current shear but also depends on bottom cohesive nature, which in turn depends, in poorly understood way, on clay mineralogy and on the geochemistry and microbiological processes occurring in the bottom. The amount of fine grained sediment eroded from a cohesive sediment bed is given by Gailani et al. (1991) as :

$$\varepsilon=\frac{a_0}{T_d^m}\left(\frac{\tau_b-\tau_c}{\tau_c}\right)^n, \quad (13)$$

where ε denotes erosion potential ($mg\,cm^{-2}$), a_0 a constant depending upon the bed properties ($=2.1\,mg\,cm^2$), T_d a time after deposition (days), τ_b bed shear stress ($dynes\,cm^{-2}$), τ_c critical shear stress for erosion ($=1.0\,dynes\,cm^{-2}$), m ($=0.5$)

Table 1. The amplitudes and phase (referenced at GMT+08.00) of the 4 dominant harmonic constituents along the open boundary from tide prediction model ORI. 96.

Constituent	Amplitude and Phase	Sta. 1	Sta. 2	Sta.3	Sta.4	Sta.5
M_2	Amplitude (m)	0.699	0.699	0.699	0.646	0.647
	Phase (deg)	276.88	276.04	276.04	278.38	278.37
S_2	Amplitude (m)	0.465	0.468	0.468	0.478	0.478
	Phase(deg)	322.57	322.54	322.54	322.57	322.50
K_1	Amplitude (m)	0.221	0.224	0.224	0.211	0.211
	Phase (deg)	159.02	160.27	160.27	156.66	156.40
O_1	Amplitude (m)	0.164	0.165	0.165	0.159	0.159
	Phase (deg)	139.36	140.45	140.45	137.22	137.03

and n (=2.5) constants dependent upon the depositional environment.

The deposition model

The deposition rate for cohesive sediments is calculated according to the formulation of Krone (1962) as follows:

$$D_d = -W_s C P_d, \tag{14}$$

where D_d denotes depositional flux ($\mathrm{g\,cm^{-2}\,s^{-1}}$), and P_d probability of deposition described by,

$$P_d = 1 - \left(\frac{\tau_b}{\tau_d}\right) \quad \text{for } \tau_b \le \tau_d, \tag{15.a}$$

$$P_d = 0 \quad \text{for} \quad \tau_h < \tau_d, \tag{15.b}$$

where τ_d is the critical shear stress for deposition (=1.0 dynes $\mathrm{cm^{-2}}$).

Settling speeds of cohesive flocs have been measured over a large range of concentrations and shear stresses (Burban et al., 1990). Experimental results show that the settling speed of cohesive flocs is dependent on the product of concentration and the water column shear stress at which the flocs are formed, resulting in the following relationship:

$$W_s = \alpha (CG)^{\beta} \tag{16}$$

in which W_s, C, and G are expressed in $\mathrm{m\,day^{-1}}$, $\mathrm{mg\,l^{-1}}$, and dynes $\mathrm{cm^{-2}}$, respectively. For saltwater suspensions, analysis of Burban et al. (1990) data revealed values of α and β of 2.42 and 0.22, respectively. The above equation implicitly incorporates the effect of internal shear stress (G) on aggregation and settling. The water column stress (G) is computed from the hydrodynamic output (i.e., current velocity and vertical eddy viscosity) as follows:

$$G = \rho A_V \left[\left(\frac{\partial u}{\partial z}\right)^2 + \left(\frac{\partial v}{\partial z}\right)^2 \right]^{1/2} \tag{17}$$

Table 2. The salinity and temperature along the open boundary.

Station	Temperature (°C)			Salinity (PSU)		
	$\Delta\sigma_1$	$\Delta\sigma_2$	$\Delta\sigma_3$	$\Delta\sigma_1$	$\Delta\sigma_2$	$\Delta\sigma_3$
Sta. 1	28.14	27.03	24.11	32.04	32.05	34.33
Sta. 2	28.04	27.21	23.64	33.55	33.94	35.00
Sta. 3	28.04	27.23	23.32	33.05	33.07	33.08
Sta. 4	28.06	27.12	24.20	33.25	33.61	33.97
Sta. 5	28.16	27.05	23.88	21.01	21.01	21.02

$\Delta\sigma_1 = \Delta\sigma_2 = \Delta\sigma_3$ = the sigma level

Boundary and Initial Conditions

The boundary condition along the open boundary obtained by the linear interpolation at five points (1, 2, 3, 4, 5) with star marks (see Fig. 1b), was given as the tidal elevation, salinity, temperature, and suspended sediment concentration. The tidal elevation used harmonic constant of M_2, S_2, K_1 and O_1 constituents given by ORI. 96 model are shown in Table 1. ORI.96 ocean tide model was developed at Ocean Research Institute, University of Tokyo. The ORI. 96 model provides grid values of harmonic constants of pure ocean tide (0.5×0.5 degrees) and radial loading tide (1×1 degrees) for 8 major constituents (Matsumoto et al., 1995). The salinity and temperature obtained from Levitus 94 (http://www.nodc.noaa.gov) are shown in Table 2. The SSC was set with 1 mg $\mathrm{l^{-1}}$, which was obtained by field measurement, along the open boundary.

The river discharge at the upstream boundary in June and July 2003 of 2040 $\mathrm{m^3\,s^{-1}}$ was given at Sebulu in Fig. 1(b). The averaged monthly river discharge data of the Mahakam river (1993–1998) obtained from the Research and Development Irrigation Ministry Public Work, Republic of Indonesia are shown in Fig. 2. Temperature, salinity, and SSC at the upstream boundary under river discharge were 290C, 0.1 psu, and 170 $\mathrm{mg\,l^{-1}}$, respectively. The sediment concentration obtained from Allen et.al., (1977) was given and the average sediment discharge is estimated at 8×10^6 $\mathrm{m^3\,yr^{-1}}$, although this number is not based on actual field measurement but on volumetric calculations.

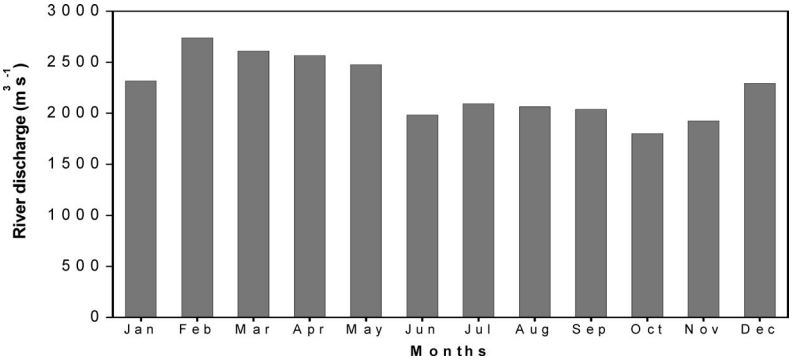

Fig. 2. The monthly river discharge ($m^3\,s^{-1}$) data of the Mahakam river (1993–1998).

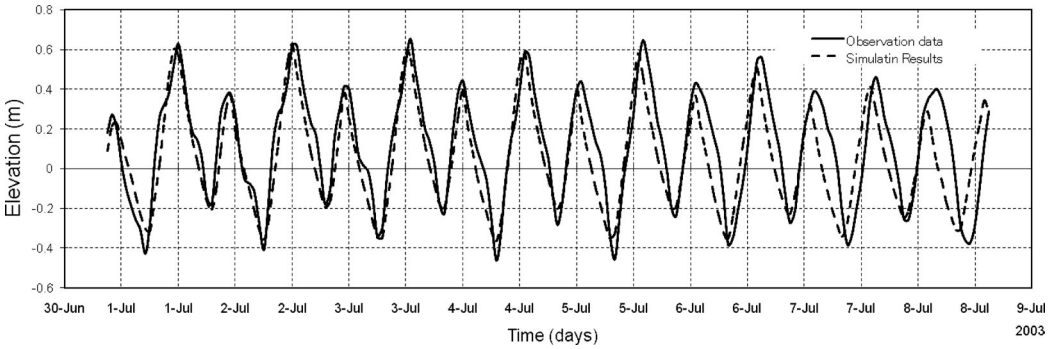

Fig. 3. Verification of elevation between the observation data (IMAU Utrecth Univ.) and the simulation results at Muara Jawa for the period of 1 to 8 July 2003.

The initial conditions of temperature and salinity are necessary for the start of the simulation. The temperature and salinity at offshore area are obtained from Levitus 94, meanwhile at Mahakam delta and river area were obtained from observation results (IMAU). The initial SSC was set to be 5 $mg\,l^{-1}$.

Numerical experiment

In the model application, the water body is discritized by 3 equal layers over the depth. The horizontal grid size is 200 m, resulting in 468×490 grids covering the study area. In the numerical experiment, the surface wind stress is neglected. The maximum time step lengths for obtaining convergent numerical results are: Δt_E (external mode time step length)=4 s, Δt_I (internal mode time step length)=40 s. The model was originally set up to simulate the period between June 27, 2003 and July 12, 2003 and verified against extensive field observation data including water surface elevation, current velocities, SSC, salinity, and temperature.

Results

Tide and Current

The comparison of the observed water elevation data at Muara Jawa with the model results for corresponding 8 days (1–8 July 2003) is shown in Fig. 3. The root mean squared (RMS) error between the model results and the observed ones is 0.15 m.

Figure 4 shows the current verification of simulation results with observation data conducted at Muara Jawa. Figure 4 shows that eastward component of current velocity (positive value) has an appropriate phase with observation data in almost every condition with the RMS error of 0.04 $m\,s^{-1}$.

Temperature, salinity, and density

Figure 5 shows the comparison of the observed vertical distribution of temperature and simulated one along the Mahakam river main channel from Muara Jawa to Muara Pegah on 6 July during neap tide condition. The observed temperature was dropping in seaward direction. A clear wedge of fresh warm river water floats on the saline cold seawater. The simulation results show that the temperature starts to decrease about at 33 km from Muara Jawa.

Figure 6 shows the results of the observed and simulated salinity distributions along the main channel from Muara Jawa to Muara Pegah. The observed salinity clearly shows the fresh water–salt water interface. The salinity starts to increase about at 30 km from Muara Jawa. Most of the mixing occurs between 30 km and 40 km from Muara Jawa. The simulation results show the vertical profile of developed salt wedge due to freshwater influx from the river out to the

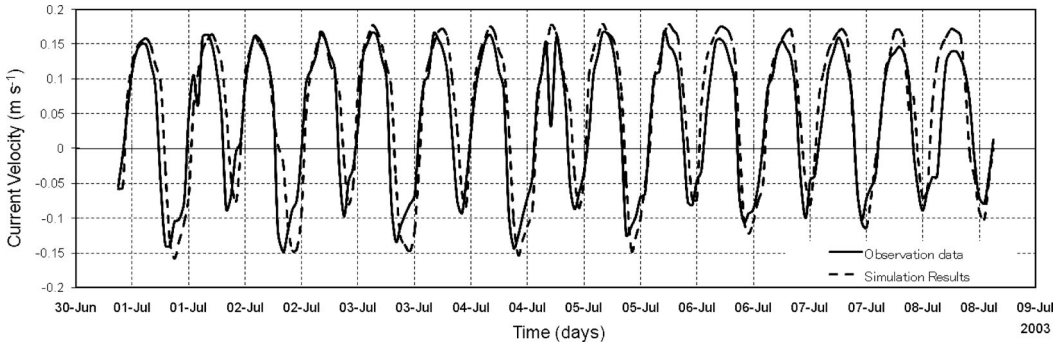

Fig. 4. Verification of the current velocity component U (x direction, eastward (+) − westward (-)) between the observation data (IMAU Utrecht Univ.) and the simulation results at Muara Jawa at the depth of 4.0 m from the surface for the period of 1 to 8 July 2003.

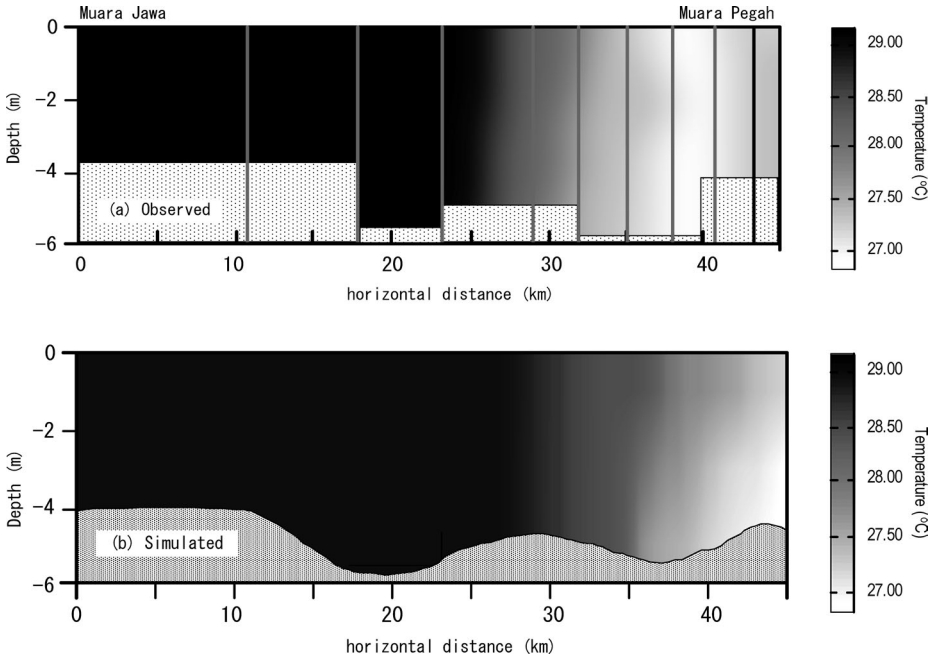

Fig. 5. Comparison of the vertical distributions of observed and simulated temperature along the Mahakam river from Muara Jawa to Muara Pegah on 6 July 2003 during neap tide condition. (a) the observation results and (b) the simulation results.

ocean in neap tide condition.

The observation showed a full mixed distribution of salinity along the river, with a range from 25 psu near the river mouth to 5 psu near the upstream end of the main river channel. These observed features were well captured in the model simulation.

Figure 7 shows the observed and simulation results of sigma-t (density) distributions on 6 July during neap tide condition. The vertical distribution of density shows the same pattern as salinity along the main channel from Muara Jawa to Muara Pegah. The temperature effect is less than that of salinity to the density distribution. This implies that the density variation is dominated by the salinity variation. The presence of salty ocean water at downstream end and freshwater at the upstream results in spatial salinity (and hence density) gradient. This causes a gravitational circulation with the salty water moving upstream in the lower layer and fresh water moving downstream in the surface layer. The vertical density gradient stabilizes the water column, which inhibits vertical mixing (Fig. 7).

Suspended Sediment

Measurement of the SSC in the Mahakam estuary during 1 to 8 July 2003 were used to verify the cohesive sediment transport model. The data were provided by IMAU, Utrecht University, the Netherland. Figure 8 shows the verification of SSC between the observation data and the simulation results at Muara Jawa (Fig. 1(b)). The SSC simulation result shows lower values than the observation data on 1 July during spring tide condition, but on the contrary a little higher ones on 6 July during neap tide condition. The simulation results were compared with available suspended sediment concentration with RMS error of 33.11 mg l^{-1}.

Figure 9(a) and (b) show the results of observed and

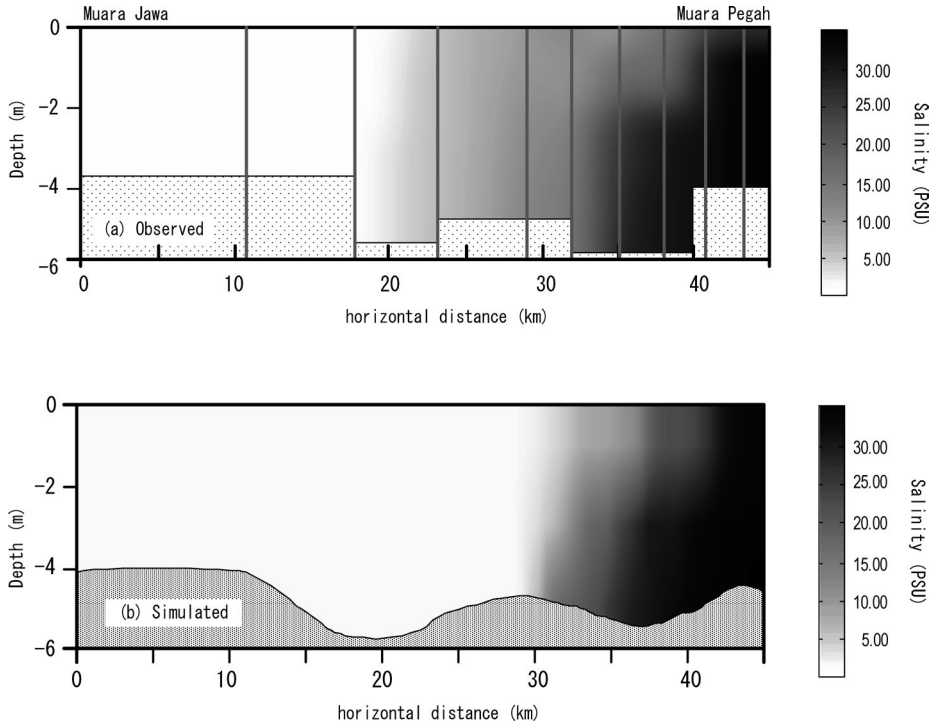

Fig. 6. Comparison of the vertical distributions of observed and simulated salinity along the Mahakam river from Muara Jawa to Muara Pegah on 6 July 2003 during neap tide condition. (a) the observation results and (b) the simulation results.

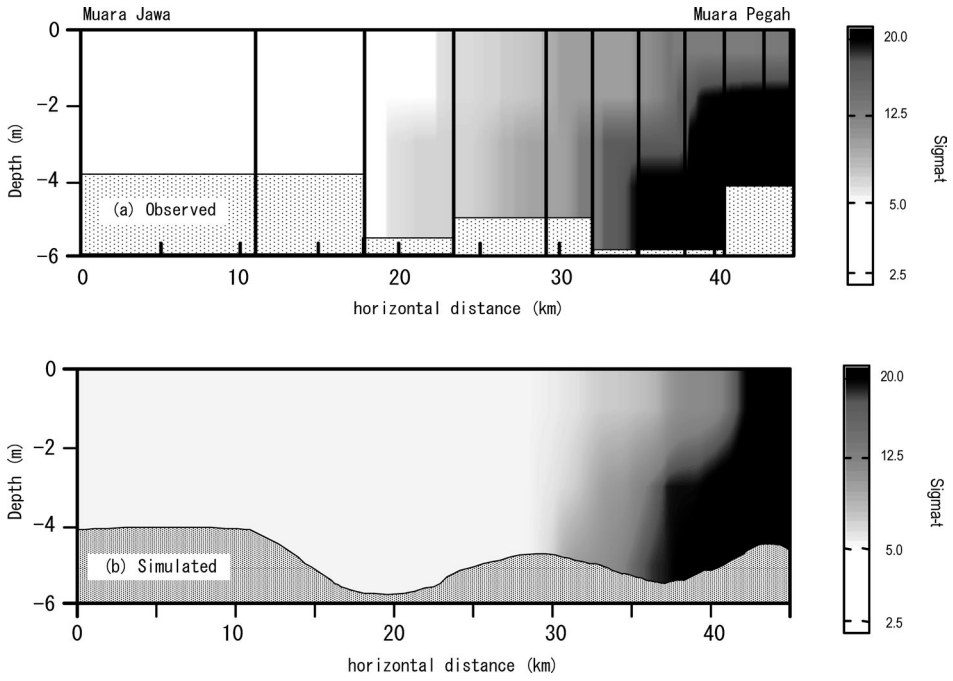

Fig. 7. Comparison of the vertical distribution of observed and simulated density (sigma-t) along the Mahakam river from Muara Jawa to Muara Pegah on 6 July 2003 during neap tide condition. (a) the observation results and (b) the simulation results.

simulated spatial distributions of SSC in the Mahakam river between Muara Jawa and Muara Pegah on 6 July 2003 during neap tide condition. The observed SSC is decreasing sharply between 30 and 35 km from Muara Jawa (Fig. 9(a)). Figure 9(b) shows the result of simulated SSC which starts to decrease at 30 km from Muara Jawa. Sudden increases in SSC are visible at 35–40 km from Muara Jawa. The reason of low SSC between 30 and 40 km from Muara Jawa is due to low current velocity there. The large current velocity in the near bottom layer at the tip of salt wedge area decreases due to

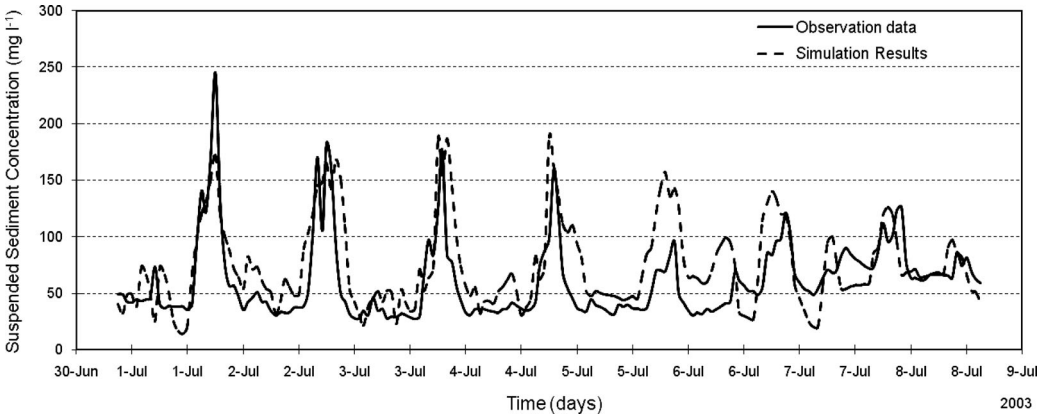

Fig. 8. Verification of suspended sediment concentration (SSC) between the observation data (IMAU Utrecht Univ.) and the simulation results at Muara Jawa at depth of 4.0 m from the surface for the period of 1 to 8 July 2003.

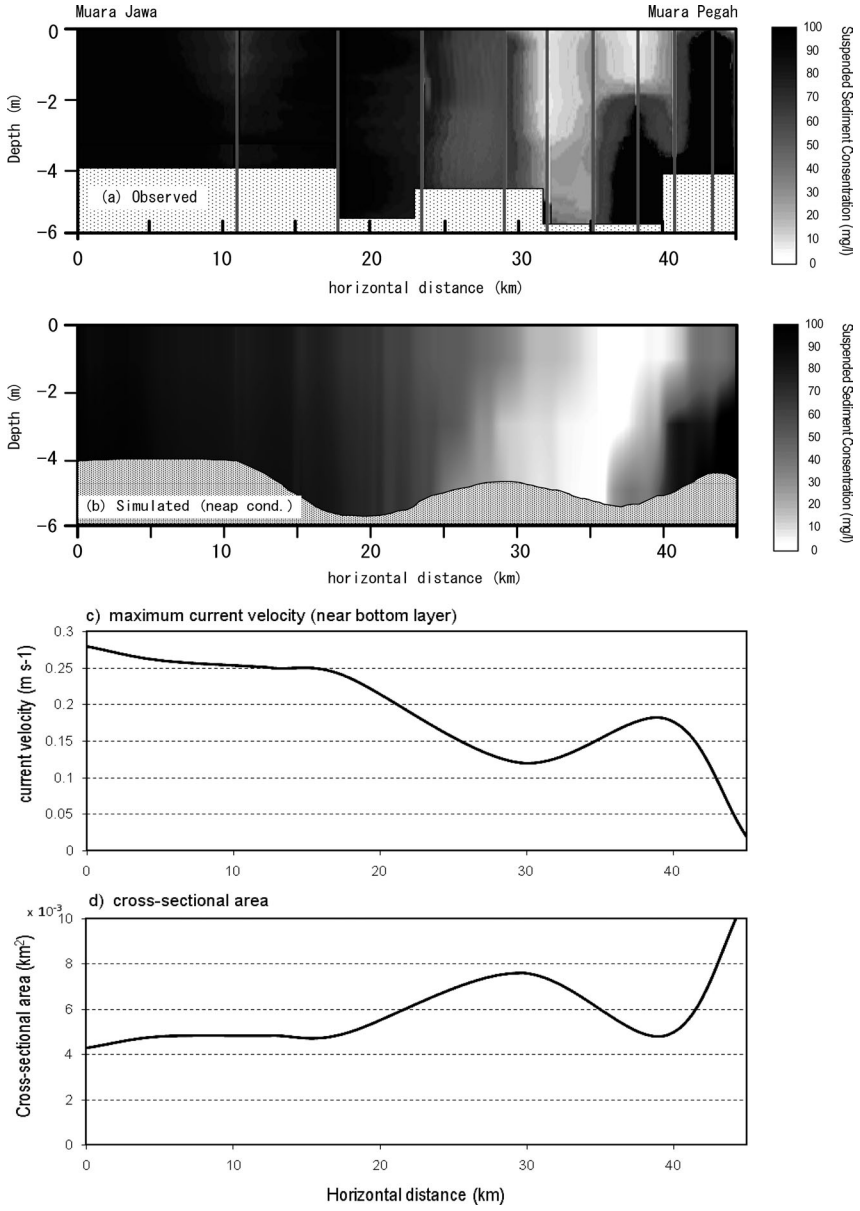

Fig. 9. Comparison of the vertical distributions of observed and simulated suspended sediment concentration on 6 July 2003 during neap tide condition. (a) the observation results, (b) the simulation results, (c) the maximum current velocity (near bottom layer), and (d) the cross-sectional area.

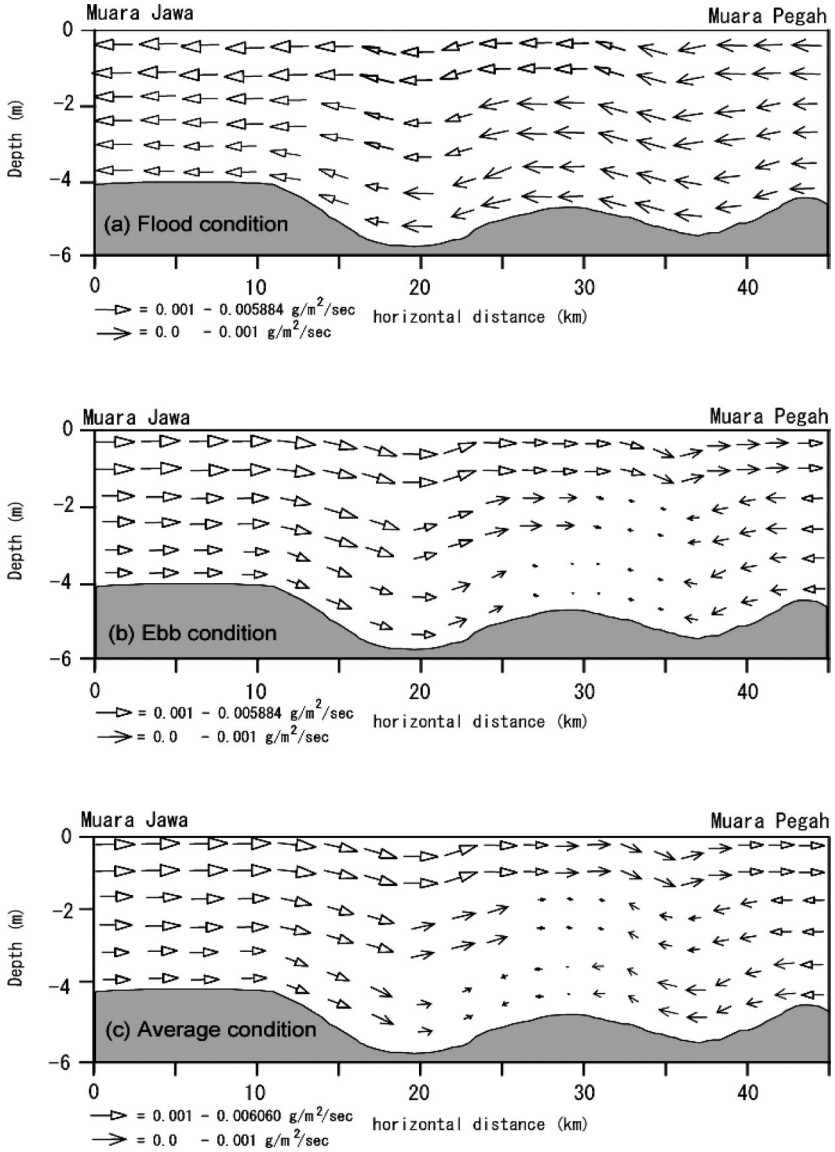

Fig. 10. Profile of cohesive sediment transport during neap tide condition at (a) flood, (b) ebb, and (c) average.

large cross sectional area around 30 km from Muara Jawa as shown in Fig. 9(c) and (d).

The behavior of suspended sediment varies depending on circulation pattern resulting from the relative importance of tidal current effect to river discharge. The vertical distributions of suspended sediment transport by 3D hydrodynamic baroclinic simulation during flood, ebb, and average in neap tide condition, respectively, are shown in Fig. 10. During the flood condition, the suspended sediment is transported to upstream. The minimum suspended sediment transport in the Muara Pegah is 0.001 g/m^2/sec and increase to 0.005884 g/m^2/sec towards upstream (Muara Jawa) (Fig. 10(a)). During the ebb condition, the pattern of suspended sediment transport in the opposite direction with flood condition, but the upstream suspended sediment transport in the lower layer is seen between 27 and 45 km from Muara Jawa (Fig. 10(b)). The position of salt wedge is pushed offshore, because more sediment is transported directly to offshore area. For average condition (Fig. 10(c)) during one tidal cycle in the river mouth, net flow in the lower (salty) layer is directed toward the river head of the delta until 30 km from Muara Jawa, while net flow in the upper (fresh) layer directed toward the sea. Suspended sediment, transported to the delta from the upland, may be carried upstream when it settles into the lower layer, finally being deposited at the tip of the salt wedge. The tip of salt wedge is located in the main river channel between 30 and 35 km from Muara Jawa.

Figure 11(a) shows the simulation results of vertically-averaged transport of suspended sediment at maximum flood on 6 July 2003 in neap tide condition. The suspended sediment is transported from the offshore area to delta waters until to Samarinda. In the Mahakam river area the suspended sediment is transported from upstream to downstream. The sediment transport at delta waters is 0–0.001 g/m^2/sec. when

a

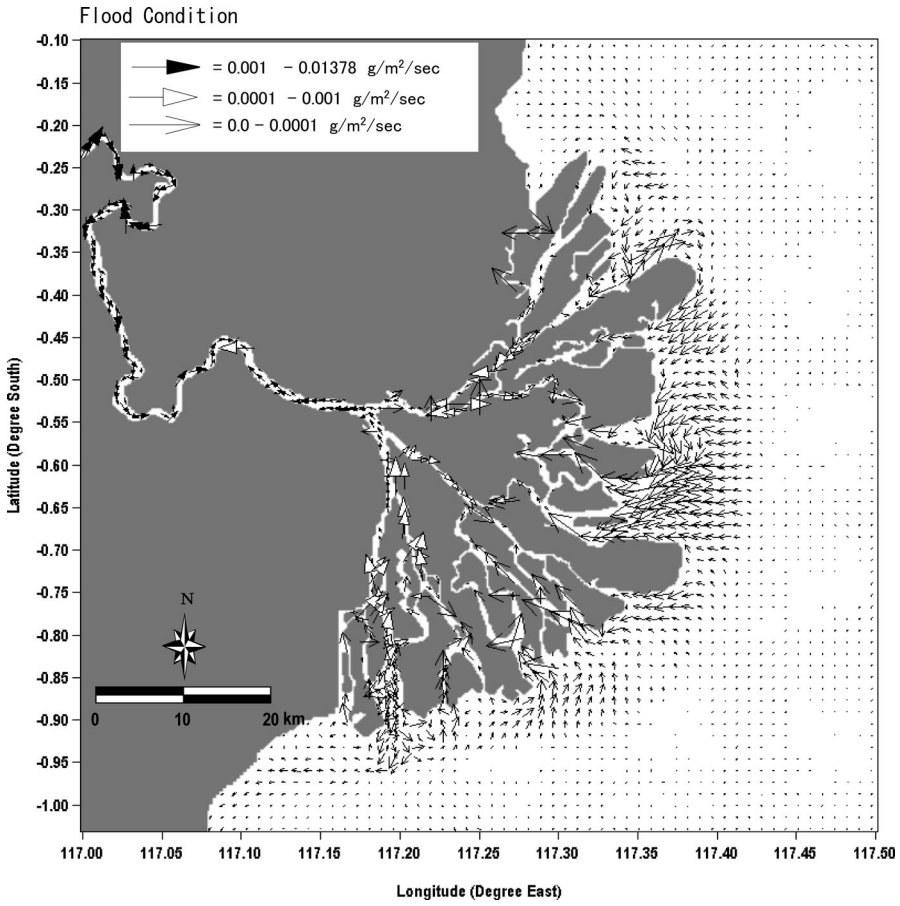
Flood Condition
= 0.001 – 0.01378 g/m²/sec
= 0.0001 – 0.001 g/m²/sec
= 0.0 – 0.0001 g/m²/sec
N
0
10
20 km.
Latitude (Degree South)
Longitude (Degree East)

b

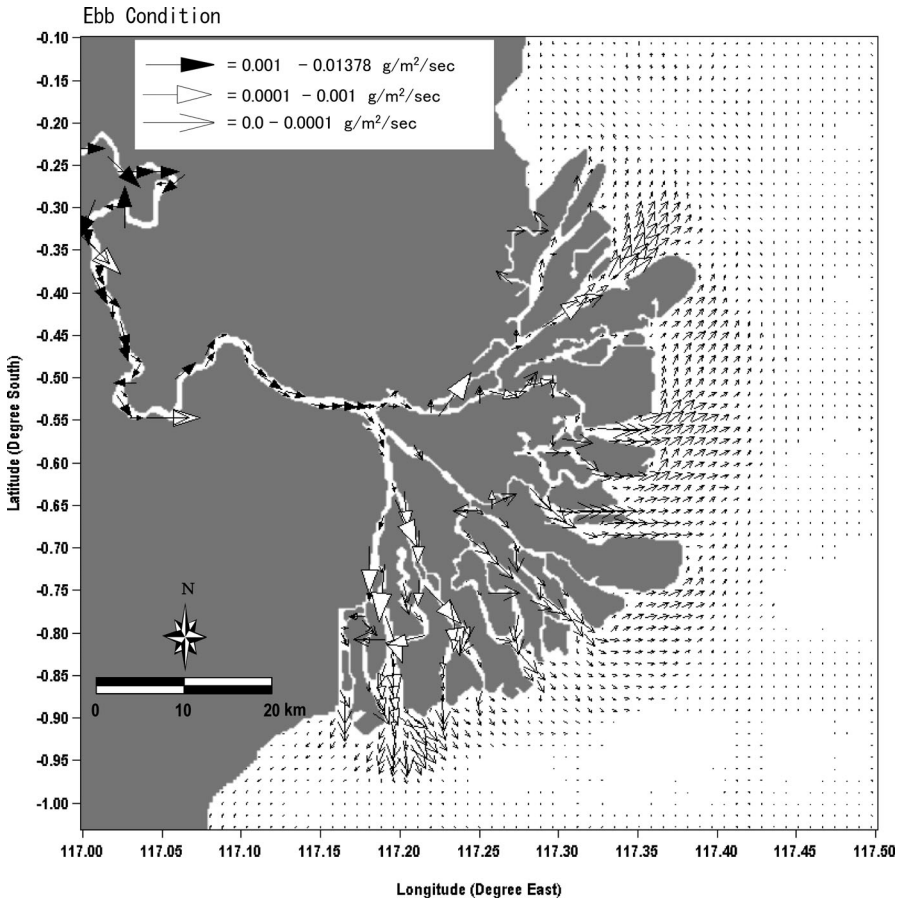
Ebb Condition
= 0.001 – 0.01378 g/m²/sec
= 0.0001 – 0.001 g/m²/sec
= 0.0 – 0.0001 g/m²/sec
N
0
10
20 km
Latitude (Degree South)
Longitude (Degree East)

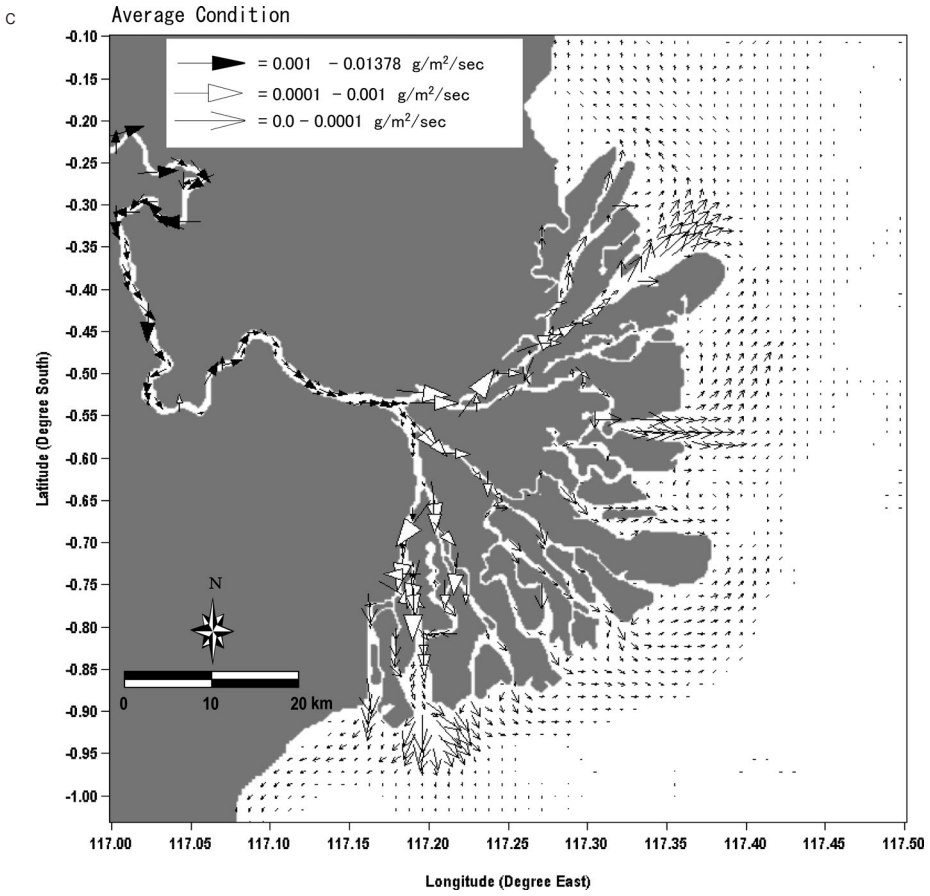

Fig. 11. The horizontal sediment transport in neap tide condition (a) during flood (b) during ebb, and (c) average.

it is transported into Mahakam river the suspended sediment transport increases about 0.001–0.01378 g/m^2/sec. During the ebb tidal condition suspended sediment is transported from the Mahakam river towards the offshore area in the whole area of the Mahakam estuary as shown in Fig. 11(b).

The simulation results of horizontal suspended sediment transport at average condition during one tidal cycle are shown in Fig. 11(c). The vertically averaged suspended sediment transport by the Mahakam river towards the delta waters is 0.001–0.01338 g/m^2/sec. In shallow offshore area ($<$5 m) the suspended sediment is deposited. The deposition of suspended sediment near Muara Pegah is larger than that near Muara Kaeli. In the deeper offshore area, the suspended sediment is transported northward in the Makassar strait and smaller than in the Mahakam river and delta area. This is due to the tide induced residual current in the Makassar strait, which flows northward in the Makassar strait to Celebes Sea (Hatayama et al., 1996).

Discussion

The coupled 3-D hydrodynamic circulation and suspended sediment model has reasonably reproduced the spatial and temporal distributions of SSC observed in the Mahakam estuary. The model includes baroclinic forces to incorporate density changes in the delta area.

The inclusion of the baroclinic term in the model for the stratified Mahakam estuary contributes to distribution pattern of suspended sediment, mainly of cohesive sediment. To reach the stability condition for large horizontal salinity gradient (i.e. density gradient) between fresh and saline water, the baroclinic ramp function is required to smooth the baroclinic acceleration term.

The corresponding sediment transport nearly follows the pattern of salinity transport. SSC near the bottom is higher than above layer since the settlement of suspended sediment, which drives SSC to accumulate in the bottom layer. Sediment from the Mahakam river is transported downstream, and because of settlement they reach lower layer and is transported back to the upstream by the flow in the lower layer to the convergence point (so called 'null point'). The null point is associated with a turbidity maximum region where SSC in the channel is greatest. It develops because suspended sediment moves towards the null point from both upstream and downstream, and because turbulent mixing of river water with brackish bottom water near the null point leads to flocculation.

Generally, the suspended sediment is mainly transported from Mahakam river towards Muara Pegah than Muara Berau

and Muara Bayur. The SSC at Muara Jawa, Muara Pegah, and Muara Kaeli is mainly influenced by river discharge, meanwhile at Muara Bayur and Muara Berau it is dominated by tidal current.

Acknowledgements

The authors would like to thank A. Tuijnder, F. Buschman, and A.J.F. Hoitink from IMAU (Institute for Marine and Atmospheric Research Utrecht) Utrecht University, the Netherlands for supplying field observation data for model calibration and for fruitful discussions.

Reference

Allen, G. P., Laurier, D. and Thouvenin, J., 1977. Sediment distribution patterns in the Mahakam delta. Proceedings Indonesian Petroleum Association, 159–178.

Allen, G. P. and Chambers, J. L. C., 1998. Sedimentation in the modern and miocene Mahakam delta. Indonesia Petroleum Association, Jakarta, Field Trip Guidebook, 236.

Blumberg, A. F. and Mellor, G. L., 1987. A description of a three-dimensional coastal ocean model. In: Coastal and Estuarine Sciences 4, Three-Dimensional Coastal Ocean Models, American Geophysical Union, Washington D.C, 1–20.

Blumberg, A. F. and Goodrich, D. M., 1990. Modeling of wind- induced destratification in Chesapeake Bay. Estuaries, 13, 1236–1249.

Burban, P. Y., Y. Xu, Y., McNeil, J. and Lick, W., 1990. Settling speeds of flocs in fresh and sea waters, J. Geophys. Res., 95(C10), 18213–18220.

Ezer, T. and Mellor G. L., 1992. A numerical study of the variability and the separation of the Gulf Stream, induced by surface atmosphere forcing and lateral boundary flows. J. Phys. Oceanography, 22, 660–682.

Gailani, J., Ziegler, C. K. and Lick, W., 1991. The transport of sediments in the fox river, J. Great Lakes Res., 17, 479-494

Galperin, B. and Mellor G. L., 1990. A time dependent, three-dimensional model of the Delaware Bay and River system, Estuarine, Coastal Shelf Sci., 31, 231–281.

Hatayama, T., Awaji, T. and Akitomo, K., 1996. Tidal currents in the Indonesian Seas and their effect on transport and mixing, J. Geophys. Res., 101(C5), 12353–12373.

HydroQual, Inc., 2002. A primer for ECOMSED, Users Manual, Mahwah, N. J. 07430, USA.

Krone, R. B., 1962. Flume studies of the transport of sediment in estuarial shoaling processes, Final Report, Hydraulic Engineering Laboratory and Sanitary Engineering Research Laboratory, University of California, Berkeley, 110 p.

Mandang, I. and Yanagi, T., 2008. Tide and tidal current in the Mahakam Estuary, East Kalimantan, Indoensia, Coastal Marine Science, (in press).

Matsumoto, K., Ooe, M., Sato, T. and Segawa, J., 1995. Ocean tide model obtained from TOPEX/POSEIDON altimetry data, J. Geophys. Res., 100(C12), 25319–25330.

Mellor, G. L. and Yamada, T., 1982. Development of a turbulence closure model for geophysical fluid problems, Rev. Geophys. Space Phys, 20, 851–875.

Roberts, H. H. and Sydow, J., 2003. Late Quaternanry stratigraphy and sedimentology of the offshore Mahakam delta, East Kalimantan (Indonesia). In: Sidi, F. H., Nummedal, D., Imbert, P., Darman, H., Posamanetier, H. W. (Eds) Tropical Deltas of Southeast Asia; Sedimentology, Stratigraphy and Petroleum Geology, SEPM Special Publication, 76, 125–145.

Storms, J. E. A., Hoogendoorn, R. M., Dam, R. A. C,. Hoitink, A. J. F. and Kroonenberg, S. B., 2005. Late-Holocene evolution of the Mahakam delta, East Kalimantan, Indonesia. Sedimentary Geology, 180, 149–166.